Supporting Information

An efficient biocatalytic oxidative dehydroaromatization approach for the construction of quinolines enabled by monoamine oxidase with molecular oxygen

Huanhuan Jin,[a] Shuyun Ju,*[a] , Haoran Yu,[a,b] Lirong Yang,[a,b] Wenlong Zheng[b] and Jianping Wu *[a,b]

[a] Institute of Bioengineering, College of Chemical and Biological Engineering, Zhejiang University, Hangzhou, 310027, People's Republic of China

Fax: (+86)-571-8795-2363; e-mail: wjp@zju.edu.cn, jushuyun@zju.edu.cn

[b] ZJU-Hangzhou Global Scientific and Technological Innovation Center, NO. 733 Jianshe San Road, Xiaoshan District, Hangzhou, Zhejiang, China, 311200

List of Contents

Supplementary Experimental Methods

Supplementary Data

Supplementary experimental methods

1. Genome mining-based library construction

The DNA sequences encoding MAO5, CHAO, MAO-N D11 (Supporting Information, Table S1) were codon-optimized and chemically synthesized (GENERALBIOL, China). The candidate amine oxidase genes from *P. putida* KT2440, *P. aeruginosa*, *P. fluorescens* Pf0-1, and *P. entomophila* str. L48 were amplified from the corresponding genome DNA of these strains via polymerase chain reaction (PCR) with a series of primers (listed in Table S2). All enzyme genes were inserted into the expression vector pET-28a (+) and subsequently transformed into *E. coli* BL21 (DE3) for expression. Multiple alignments were performed using the CLUSTALW server (https://www.genome.jp/tools-bin/clustalw) and displayed using Esprit (http://espript.ibcp.fr).

2. Expression conditions of candidate genes.

E. coli BL21 (DE3) were cultivated in 50 mL of liquid Luria-Bertani (LB) medium supplemented with antibiotics (50 μg/mL kanamycin) at 37 ℃ with shaking at 200 rpm until OD_{600} reached 0.6~0.8, and then induced by addition of IPTG (final concentration of 0.01 mM) at 18 ℃ for further 15 h.

After medium removal by centrifugation (4000 rpm, 10 min, 4 ℃), the cell pellet was washed with NaPi buffer (50 mM, pH 8.0) twice and resuspended in the same buffer. The cells were disrupted by sonication and the homogenates were centrifuged (4000 rpm, 30 min, 4 ℃) to remove the cell debris. Unless otherwise stated, the crude lysate in this study was obtained by this method. The crude lysates were used for SDS-PAGE analysis and enzymatic reaction.

3. Enzyme library screening

Reaction mixture comprising NaPi buffer (50 mM, pH 8.0), substrate **1a** (5 mM), crude extract (45.0 mg/mL), DMSO (5%, v/v) and catalase (1.0 mg/mL) in a total volume of 1 mL was incubated at 30 °C with 200 rpm shaking for 24 h. The sample was then analyzed by a HPLC method.

4. Effects of pH and temperature on *Pp*MAO

The effect of pH on enzyme activity was determined at different pH levels (6.0–9.0) in the following buffers (50 mM): NaPi (pH 6.0, 6.5, 7.0, 7.5, 8.0), Tris-HCl (pH 8.0, 8.5, 9.0) and Gly-NaOH (pH 9.0, 9.5, 10.0). The pH stability of *Pp*MAO was determined by preincubating the crude enzyme solution in different pH (6.0–10.0) buffers for 24 h at 4 ℃, followed by the analysis of the

residual activity at 30 ℃. The highest enzyme activity was taken as 100%. The effect of temperature on enzyme activity was determined at different temperatures ranging from 25 to 60 °C. The thermostability of *Pp*MAO was determined by preincubating the crude enzyme solution at different temperatures (30, 40 and 50 °C) followed by measuring the residual activity.

5. Analytical methods

Method 1 HPLC was performed with column Pntulips® QS-C18 Plus (5 μm, 4.6 × 250 mm) at 30 ℃. HPLC conditions: acetonitrile/H_2O=50/50, 313 nm UV detector.

Method 2 NMR spectra were recorded on a Bruker Avance DMX 500 spectrometer with $CDCl_3$ as solvent (500 MHz for ^1H, 126 MHz for ^{13}C).

Method 3 The ultra-performance liquid chromatography triple quadrupole time-of-flight mass spectrometry (UPLC-Triple-TOF-MS) was performed by using Agilent xdb-C18 (5 μm, 4.6 × 250 mm) column. The mobile phases are A-acetonitrile and B-water. Elution was carried out with the following linear gradient: 0 min 50% A, 15 min 50% A, 21 min 95% A, flow = 1 mL/min, the detection wavelength was 313 nm and the column temperature was 30 ℃. Electrospray ion source positive ion mode was adopted. For data processing, Peak View™ was used for qualitative analysis and Extract Ions Using Dialog (XIC).

Supplementary Data

1. Cloning, expression and characterization

1.1 Cloning and expression of candidate enzymes

Table S1. List of protein information of enzymes used in this study.

Enzyme	Source	GenBank Accession Number	Protein sequence identity (%)
MAO5	*Pseudomonas monteilii* ZMU-T01	WP_013972159.1	100
MAO-N D11	*Aspergillus niger*	3ZDN_A	-
CHAO	*Brevibacterium oxydans* IH-35A	QNH87113.1	27
CHAO Y459T	*B. oxydans* IH-35A	-	27
CHAO-3M[a]	*B. oxydans* IH-35A	-	27
*Pp*MAO	*P. putida* KT2440	WP_010953650.1	89
*Pa*MAO	*P. aeruginosa* PAO1	MBG4862111.1	30
*Pf*MAO1	*P. fluorescens* Pf01	WP_011335914.1	68
*Pf*MAO2	*P. fluorescens* Pf01	WP_011334155.1	25
*Pe*MAO	*P. entomophila* str. L48	WP_011533886.1	81

[a] CHAO-3M indicated CHAO T198F/L199S/M226F.

Table S2. Primes used in this study.

Prime name	Primers (5' to 3')
*Pp*MAO-F	TGCCGCGCGGCAGCCATATGCGTATAGCAATCATCGGCAG
*Pp*MAO-R	AGTGCGGCCGCAAGCTTTCACAGTTGCTCTCCGAAGTGC
*Pa*MAO-F	GTGCCGCGCGGCAGCCATATGTTGGGGGTGTTCAGCGC
*Pa*MAO-R	AGTGCGGCCGCAAGCTTTCAATCGAACAGGCGGGTGAAC
*Pf*MAO1-F	CGCGCGGCAGCCATATGAAAATCGCCATTATCGGCAGTGGCATC
*Pf*MAO1-R	GTGCGGCCGCAAGCTTTCACAGACTTTCTCCGAAGGCTGCGG
*Pf*MAO2-F	CCGCGCGGCAGCCATATGAGTACTGACGCCCCTCCCGA
*Pf*MAO2-R	TGCGGCCGCAAGCTTCTATGCCCGACGTAACGCG
*Pe*MAO-F	CCGCGCGGCAGCCATATGCGCATCGCCATCATCG
*Pe*MAO-R	GTGCGGCCGCAAGCTTTCACAGCCGCTCACCAAAGT

1.2 Multiple sequence alignments

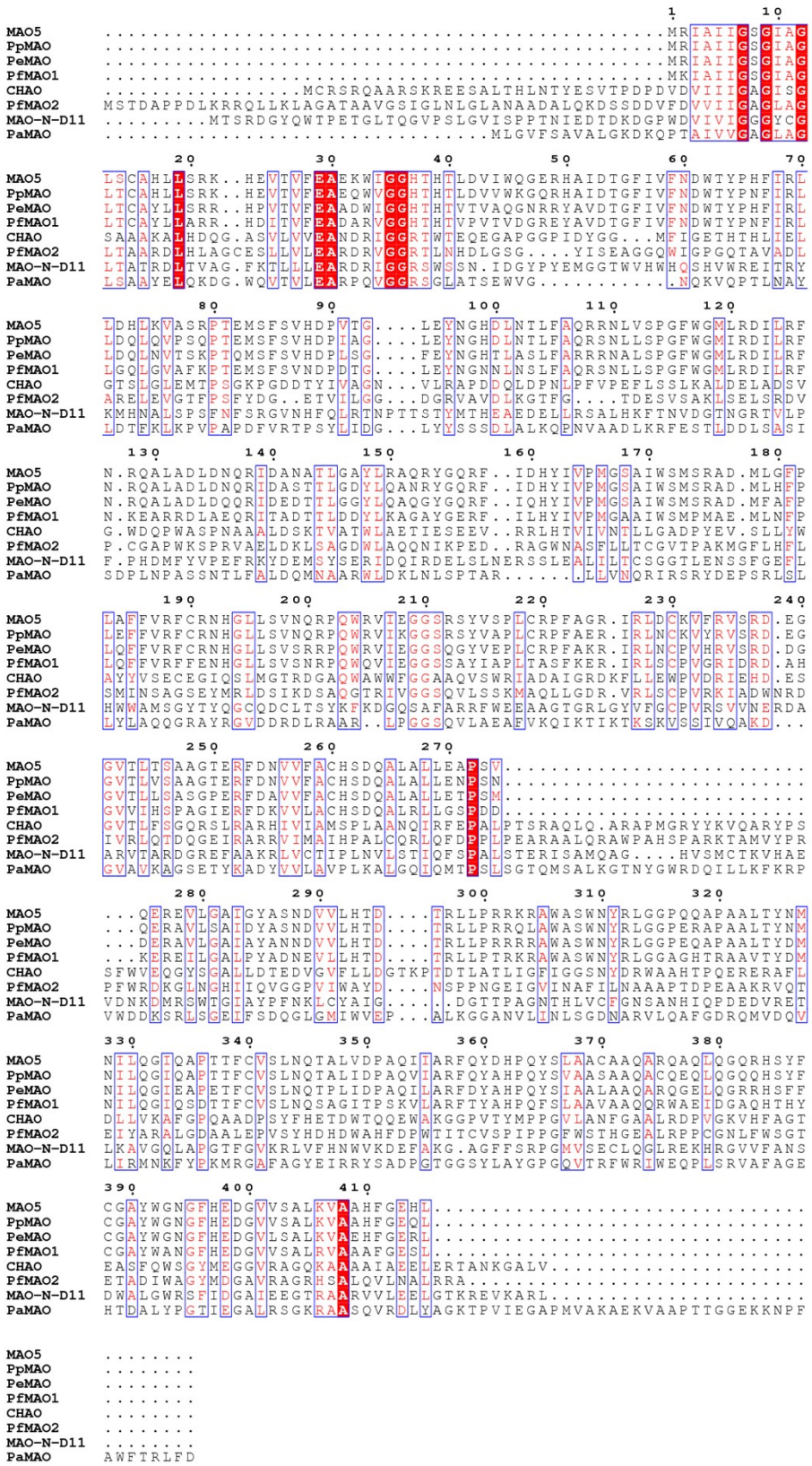

Figure S1. Multiple sequence alignments of the MAOs used in this study. Corresponding sources and GenBank accession numbers were given in Table S1. Multiple alignments were performed using the CLUSTALW server (https://www.genome.jp/tools-bin/clustalw) and displayed using Espript (http://espript.ibcp.fr).

1.3 The phylogenetic tree of amine oxidases

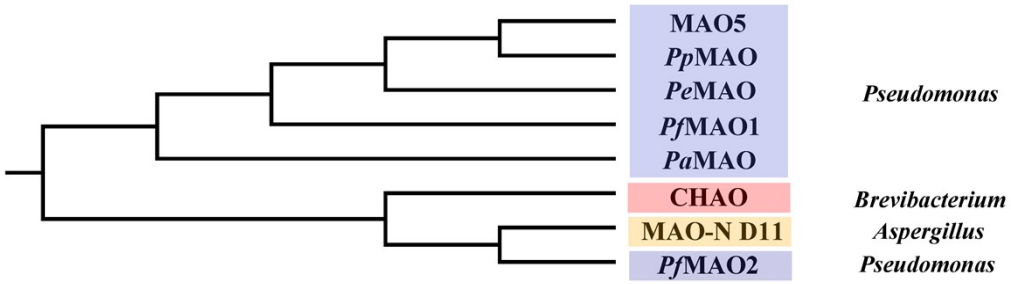

Figure S2. The phylogenetic tree of amine oxidase used in this study. The phylogenetic tree was performed using the Molecular Evolutionary Genetics Analysis Version 6.0 (MEGA 6.0).

1.4 SDS-PAGE analysis

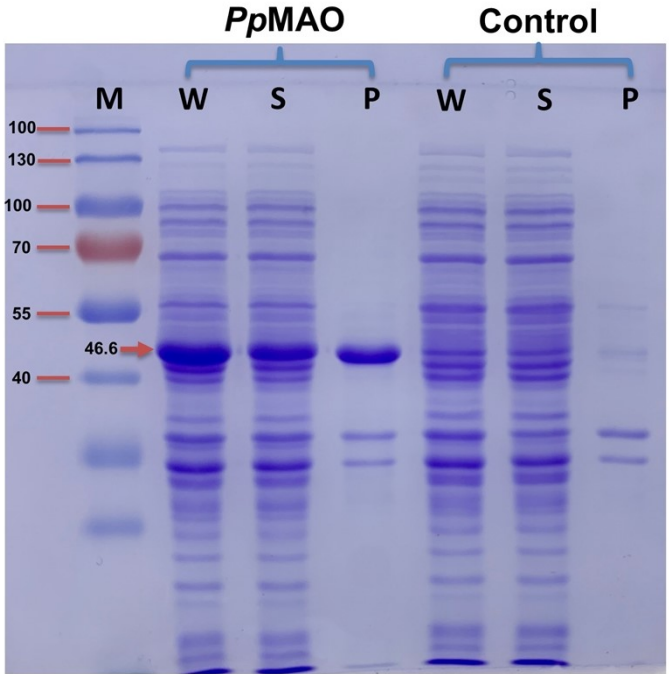

Figure S3. SDS-PAGE analysis of expression level of *Pp*MAO. Lane M, protein ruler; lane W, crude extract of whole cell; lane S, soluble fraction; lane P, precipitate (insoluble fraction). Control, *E. coli* BL21 (DE3) harboring empty plasmid pET-28a (+).

1.5 Characterization of *Pp*MAO

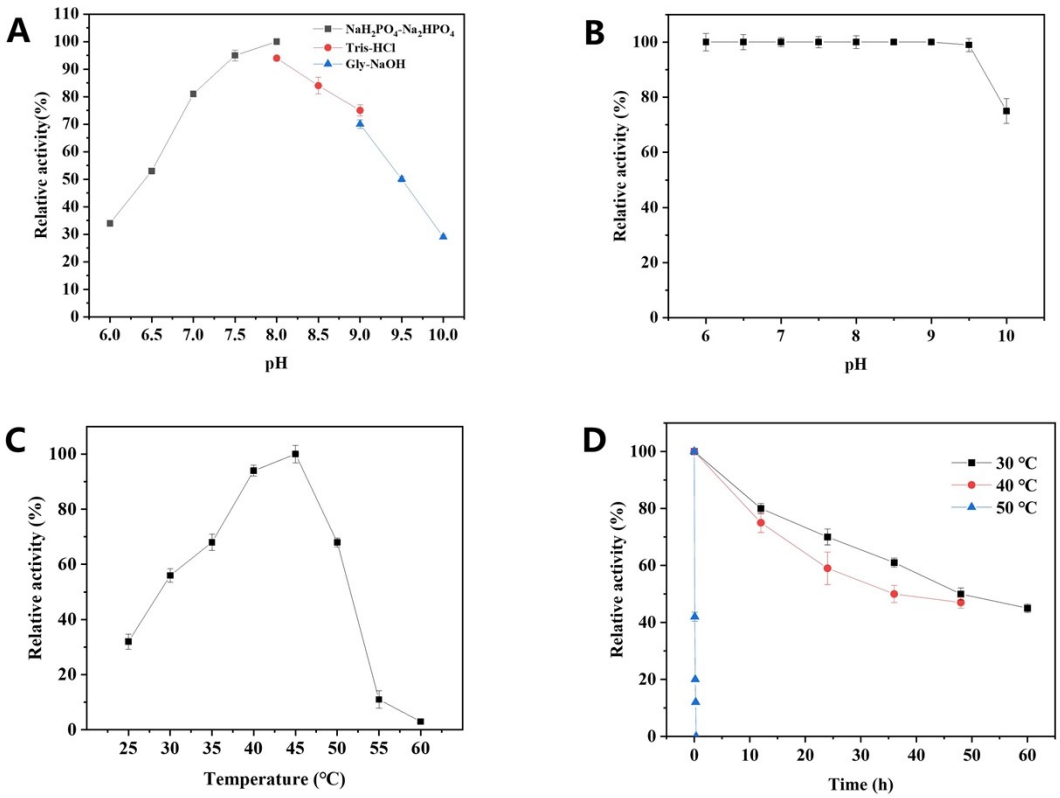

Figure S4. Effect of temperature and pH on the enzyme activity and stability of *Pp*MAO. (A) Effect of pH on the enzyme activity was determined by measuring the activity at various buffers (pH 6.0-10.0) at 30 ℃. The value at pH 8.0 was taken as 100%. (B) Effect of pH on the enzyme stability was evaluated by measuring the residual activity after incubation of the enzyme in different buffers (pH 6.0-10.0) for 24 h at 4 ℃. (C) Effect of temperature on the enzyme activity was determined by measuring the activity at various temperatures (25-60 ℃) at pH 8.0. The value at 45 ℃was set as 100%. (D) Effect of temperature on the enzyme stability was determined by measuring the remaining activity after incubation of the enzyme at 30, 40 and 50 ℃. All experiments were performed in triplicate. Each data point represents the mean ± the standard deviation of three measurements.

2. Characterization and NMR of products

2.1 Analytical data

Quinline (1b):

^{1}H NMR (500 MHz, $CDCl_3$) δ 8.91 (dd, *J* = 4.0, 1.5 Hz, 1H), 8.13 (dd, *J* = 17.2, 8.3 Hz, 2H), 7.81 (d, *J* = 8.1 Hz, 1H), 7.73 – 7.69 (m, 1H), 7.54 (dd, *J* = 11.1, 3.9 Hz, 1H), 7.39 (dd, *J* = 8.2, 4.2 Hz, 1H) ppm.

6-Methylquinoline (2b):

^{1}H NMR (500 MHz, $CDCl_3$) δ 8.83 (d, *J* = 2.9 Hz, 1H), 8.04 (d, *J* = 8.0 Hz, 1H), 7.99 (d, *J* = 8.5 Hz, 1H), 7.57 – 7.49 (m, 2H), 7.33 (ddd, *J* = 8.1, 4.1, 1.8 Hz, 1H), 2.52 (s, 3H) ppm.

6-Methoxyquinoline (3b):

^{1}H NMR (500 MHz, $CDCl_3$) δ 8.74 (dd, *J* = 4.1, 1.5 Hz, 1H), 7.99 (d, *J* = 9.2 Hz, 2H), 7.34 (ddd, *J* = 16.9, 8.7, 3.5 Hz, 2H), 7.04 (d, *J* = 2.7 Hz, 1H), 3.90 (s, 3H) ppm.

6-Hydroxyquinoline (4b):

^{1}H NMR (500 MHz, DMSO) δ 9.99 (s, 1H), 8.64 (dd, *J* = 3.9, 1.3 Hz, 1H), 8.12 (d, *J* = 8.0 Hz, 1H), 7.85 (d, *J* = 9.0 Hz, 1H), 7.38 (dd, *J* = 8.3, 4.1 Hz, 1H), 7.30 (dd, *J* = 9.0, 2.5 Hz, 1H), 7.13 (d, *J* = 2.4 Hz, 1H) ppm.

6-Fluoroquinoine (6b):

^{1}H NMR (500 MHz, $CDCl_3$) δ 8.87 (d, *J* = 2.8 Hz, 1H), 8.17 – 8.01 (m, 2H), 7.48 (td, *J* = 9.0, 2.8 Hz, 1H), 7.44 – 7.35 (m, 2H) ppm.

6-Chloroquinoline (7b):

^{1}H NMR (500 MHz, $CDCl_3$) δ 8.97 – 8.84 (m, 1H), 8.05 (dd, *J* = 13.0, 8.8 Hz, 2H), 7.80 (d, *J* = 2.1 Hz, 1H), 7.65 (dd, *J* = 9.0, 2.2 Hz, 1H), 7.42 (dd, *J* = 8.3, 4.2 Hz, 1H) ppm.

6-Bromoquinoline (8b):

^{1}H NMR (500 MHz, $CDCl_3$) δ 8.91 (dd, *J* = 4.0, 1.4 Hz, 1H), 8.05 (d, *J* = 8.1 Hz, 1H), 7.97 (dd, *J* = 5.4, 3.3 Hz, 2H), 7.77 (dd, *J* = 9.0, 2.0 Hz, 1H), 7.41 (dd, *J* = 8.3, 4.2 Hz, 1H) ppm.

7-Hydroxyquinoline (9b):

^{1}H NMR (500 MHz, DMSO) δ 10.14 (s, 1H), 8.72 (dd, *J* = 4.0, 1.4 Hz, 1H), 8.18 (d, *J* = 7.9 Hz, 1H), 7.79 (d, *J* = 8.8 Hz, 1H), 7.34 – 7.20 (m, 2H), 7.15 (dd, *J* = 8.8, 2.2 Hz, 1H) ppm.

7-Nitroquinoline (10b):

^{1}H NMR (500 MHz, $CDCl_3$) δ 9.09 (dd, *J* = 3.9, 1.4 Hz, 1H), 9.01 (d, *J* = 1.6 Hz, 1H), 8.33 (dd, *J* = 8.9, 2.2 Hz, 1H), 8.28 (d, *J* = 8.3 Hz, 1H), 7.98 (d, *J* = 8.9 Hz, 1H), 7.60 (dd, *J* = 8.3, 4.2 Hz, 1H) ppm.

6-Bromo-4-methylquinoline (11b):

^{1}H NMR (500 MHz, $CDCl_3$) δ 8.77 (d, *J* = 4.2 Hz, 1H), 8.13 (d, *J* = 2.0 Hz, 1H), 7.96 (d, *J* = 8.9 Hz, 1H), 7.76 (dd, *J* = 8.9, 2.1 Hz, 1H), 7.24 (d, *J* = 4.0 Hz, 1H), 2.66 (s, 3H) ppm.

4-Methylquinoline (12b):

^{1}H NMR (500 MHz, $CDCl_3$) δ 8.76 (d, *J* = 4.3 Hz, 1H), 8.10 (d, *J* = 8.4 Hz, 1H), 7.97 (d, *J* = 8.4 Hz, 1H), 7.73 – 7.65 (m, 1H), 7.59 – 7.50 (m, 1H), 7.20 (d, *J* = 3.9 Hz, 1H), 2.68 (s, 3H) ppm.

4-Phenylquinoline (14b):

^{1}H NMR (500 MHz, $CDCl_3$) δ 8.95 (d, *J* = 4.2 Hz, 1H), 8.18 (d, *J* = 8.4 Hz, 1H), 7.93 (d, *J* = 8.4 Hz, 1H), 7.79 – 7.69 (m, 1H), 7.62 – 7.41 (m, 6H), 7.34 (d, *J* = 4.3 Hz, 1H) ppm.

2-Methylquinoline (15b):

^{1}H NMR (500 MHz, $CDCl_3$) δ 8.02 (dd, *J* = 8.2, 5.2 Hz, 2H), 7.76 (d, *J* = 8.1 Hz, 1H), 7.67 (t, *J* = 7.7 Hz, 1H), 7.47 (t, *J* = 7.5 Hz, 1H), 7.28 (s, 1H), 2.74 (s, 3H) ppm.

2.2 ^{1}H NMR of products

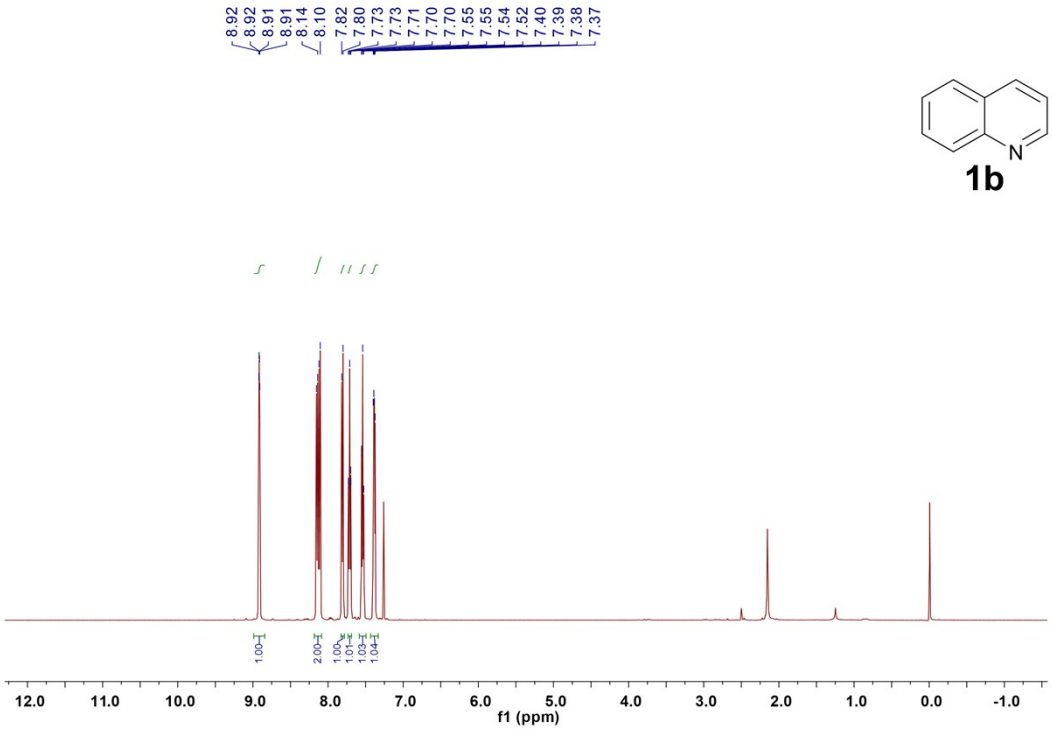

Figure S5. ^{1}H-NMR spectrum of **1b**

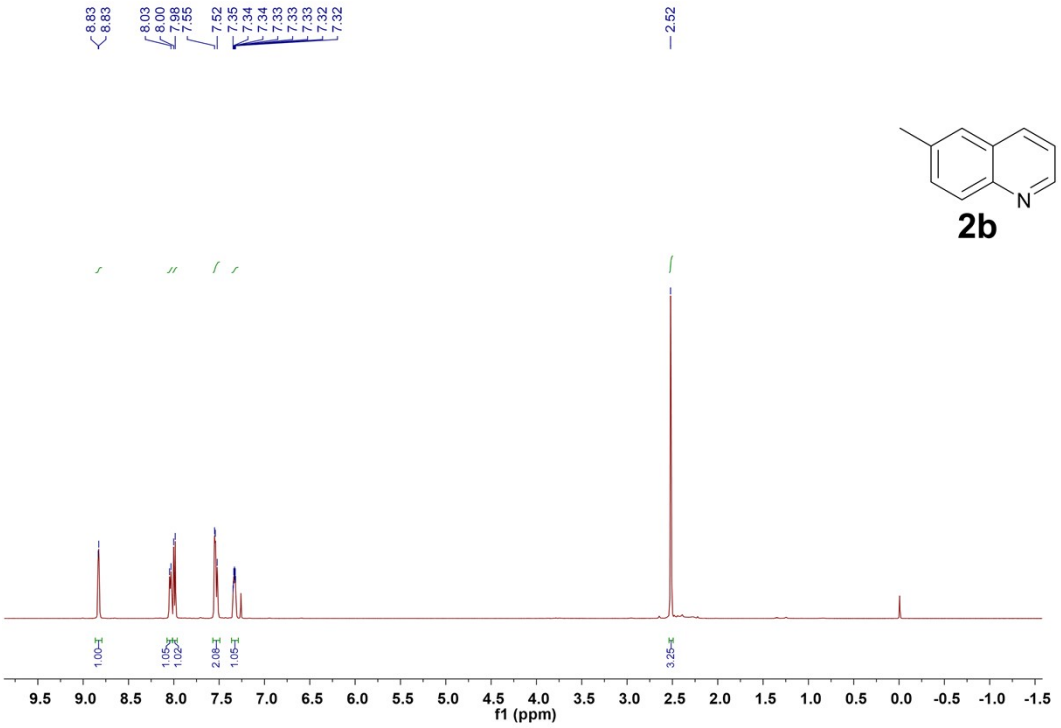

Figure S6. ^{1}H-NMR spectrum of **2b**

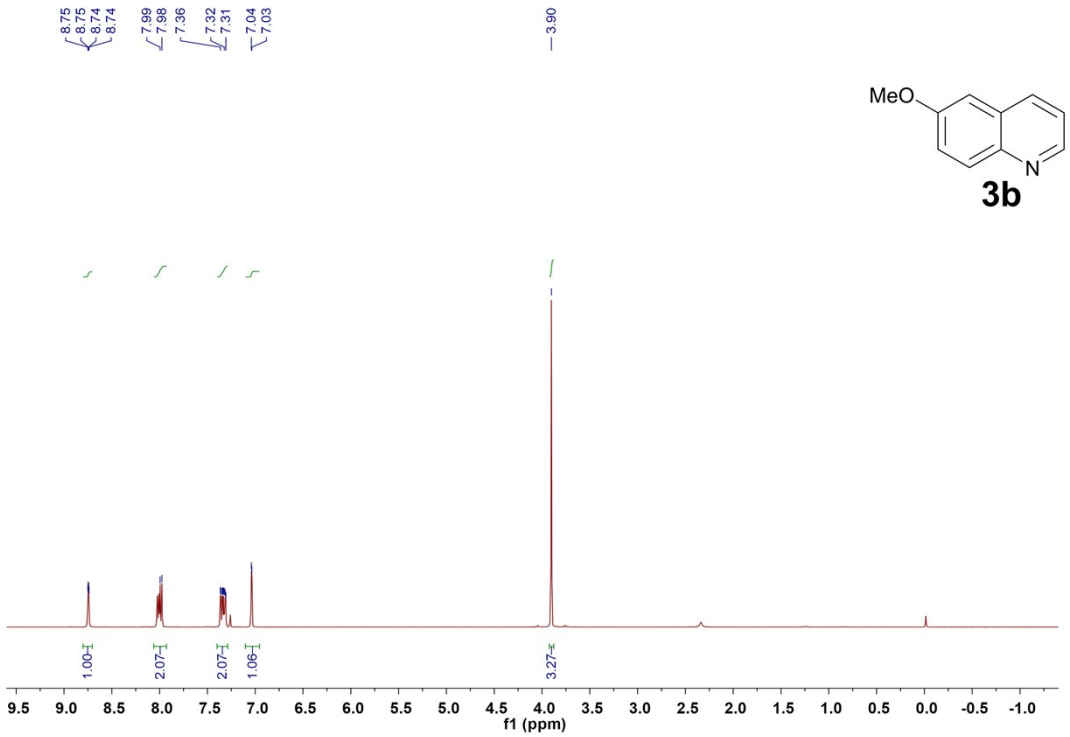

Figure S7. ^{1}H-NMR spectrum of **3b**

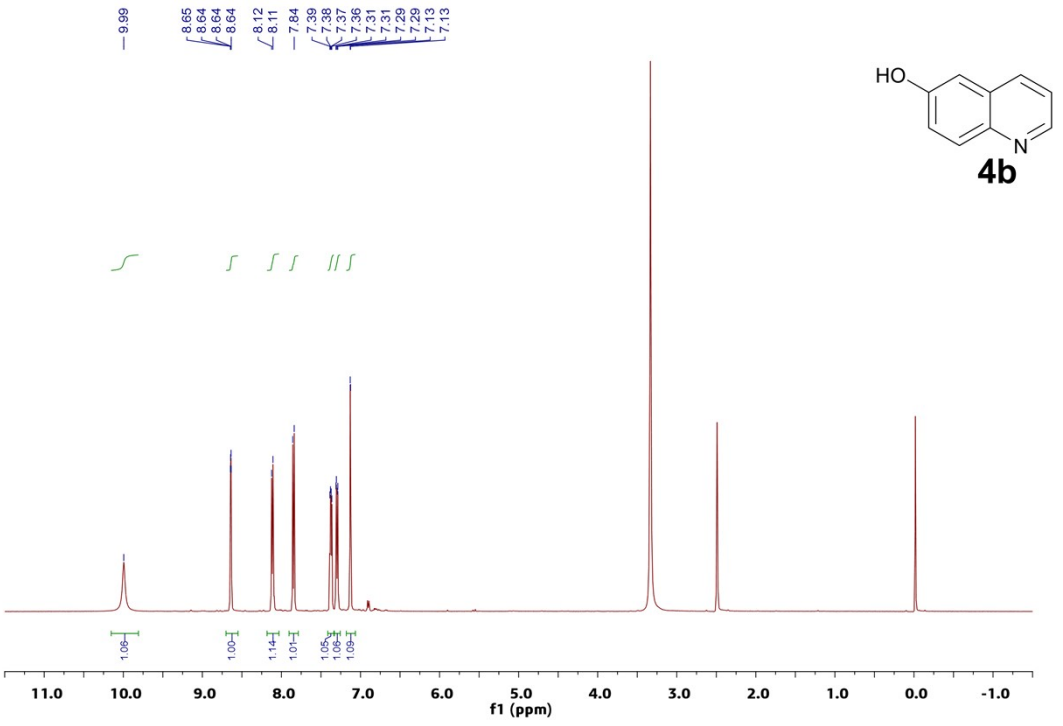

Figure S8. ^{1}H-NMR spectrum of **4b**

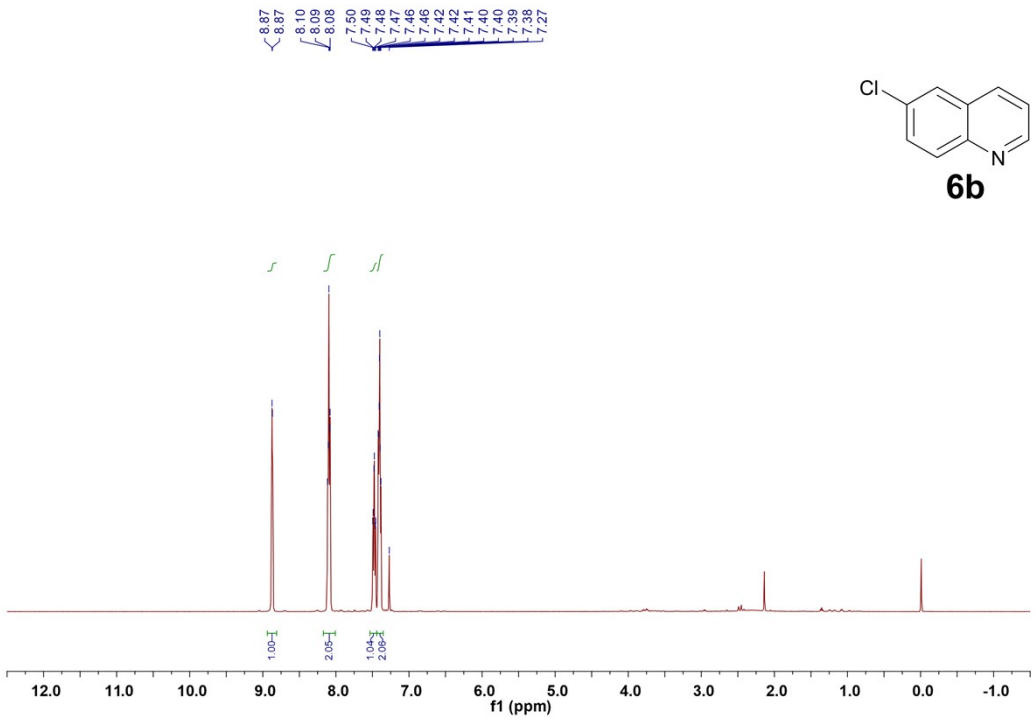

Figure S9. [1]H-NMR spectrum of **6b**

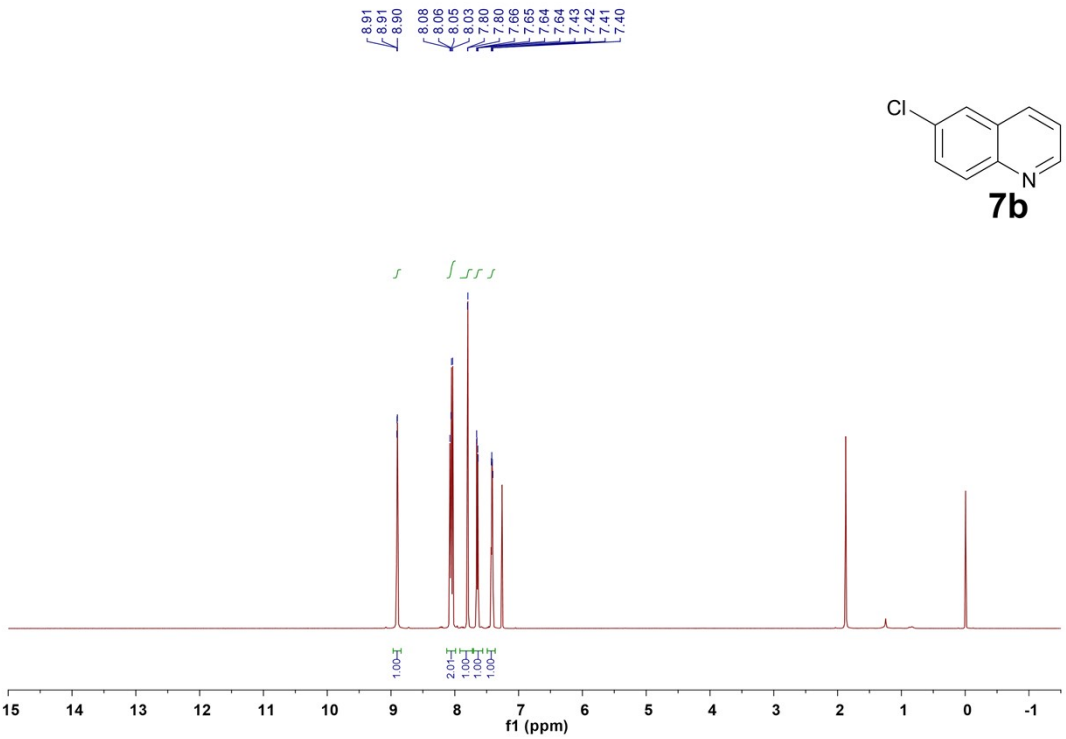

Figure S10. [1]H-NMR spectrum of **7b**

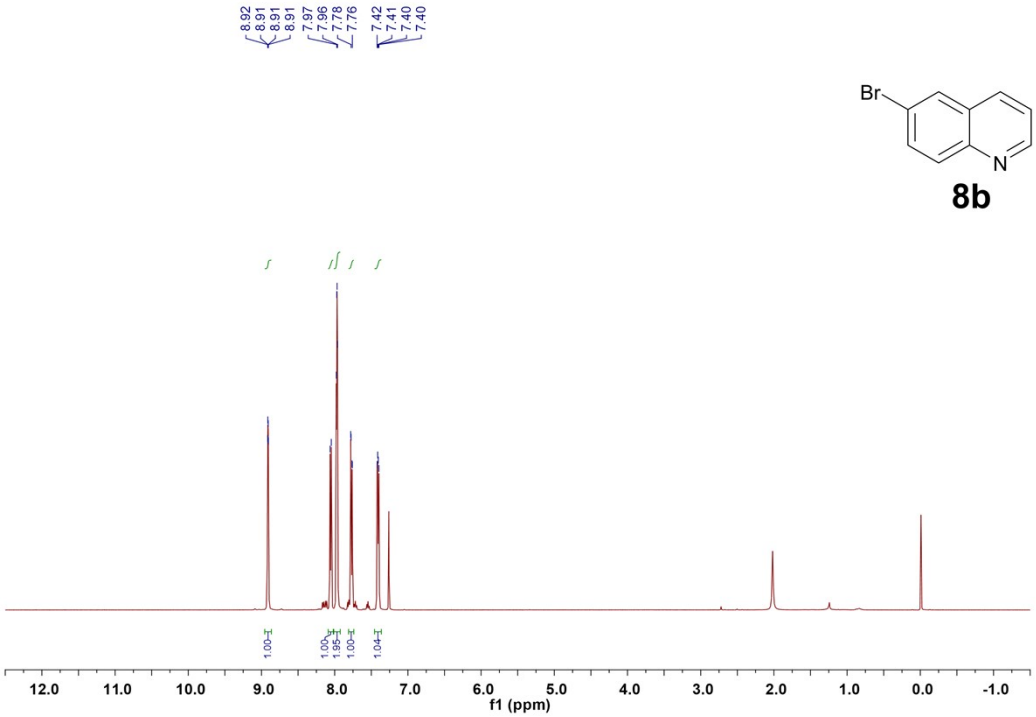

Figure S11. ^{1}H-NMR spectrum of **8b**

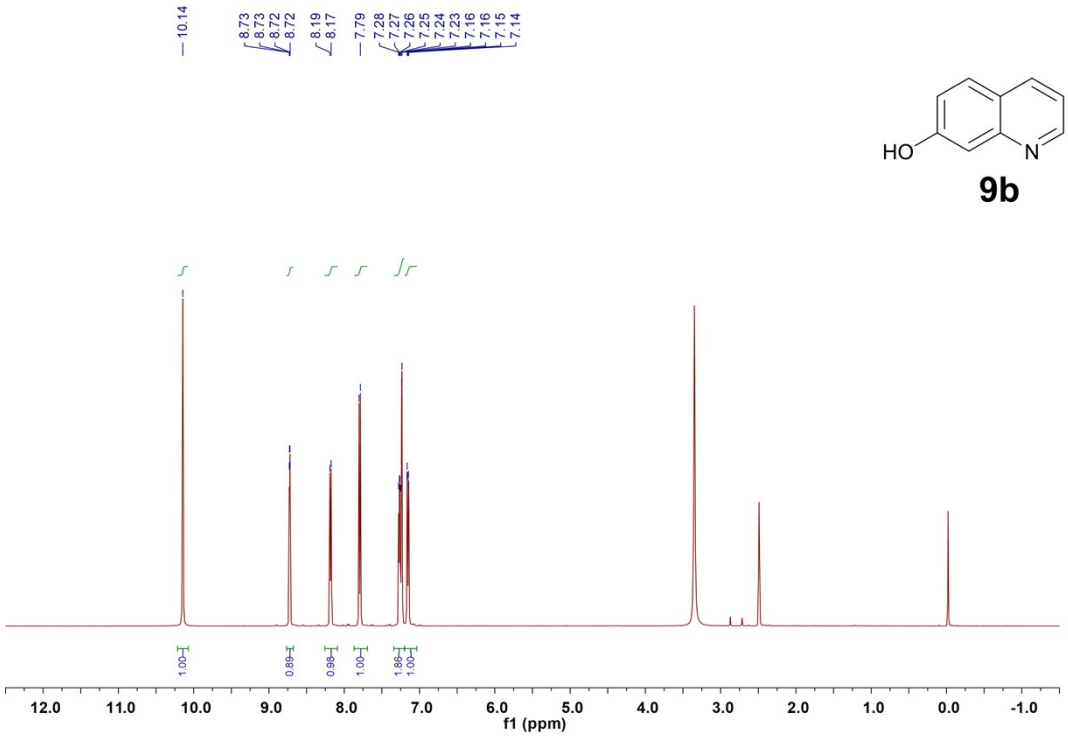

Figure S12. ^{1}H-NMR spectrum of **9b**

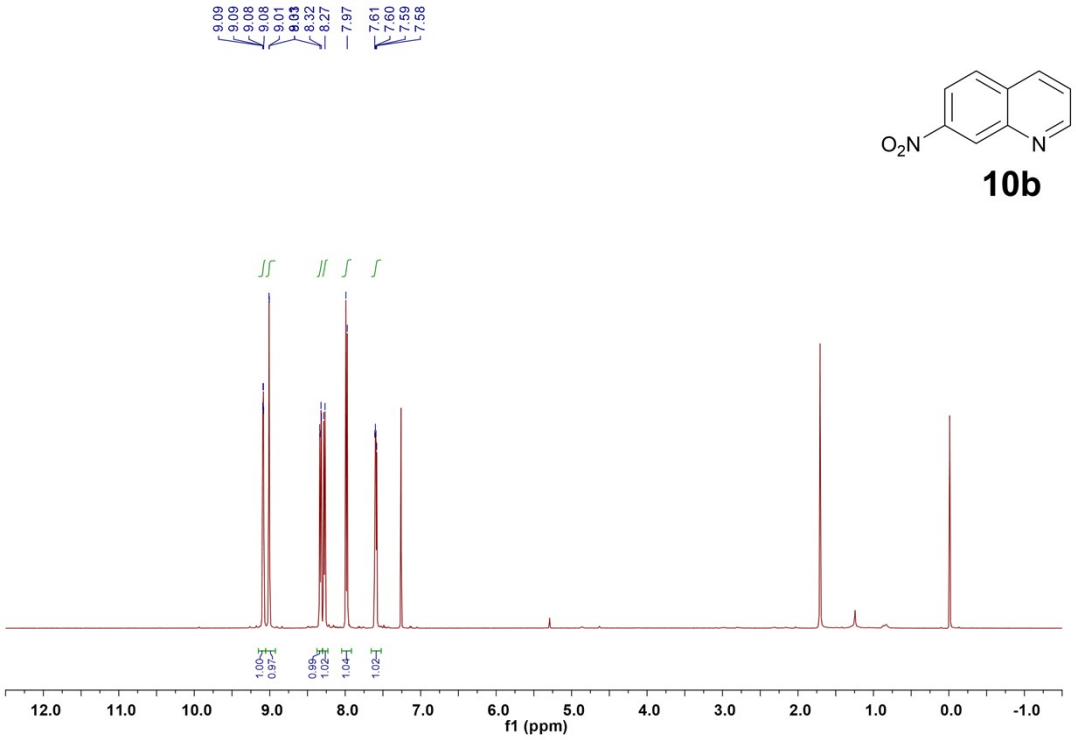

Figure S13. ^{1}H-NMR spectrum of **10b**

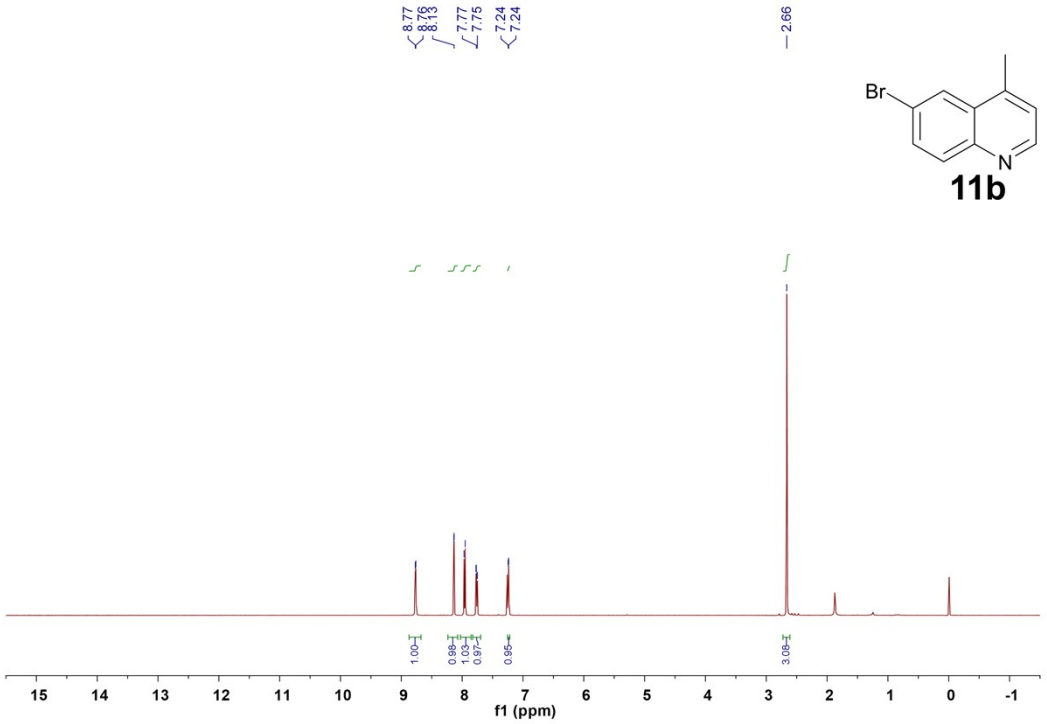

Figure S14. ^{1}H-NMR spectrum of **11b**

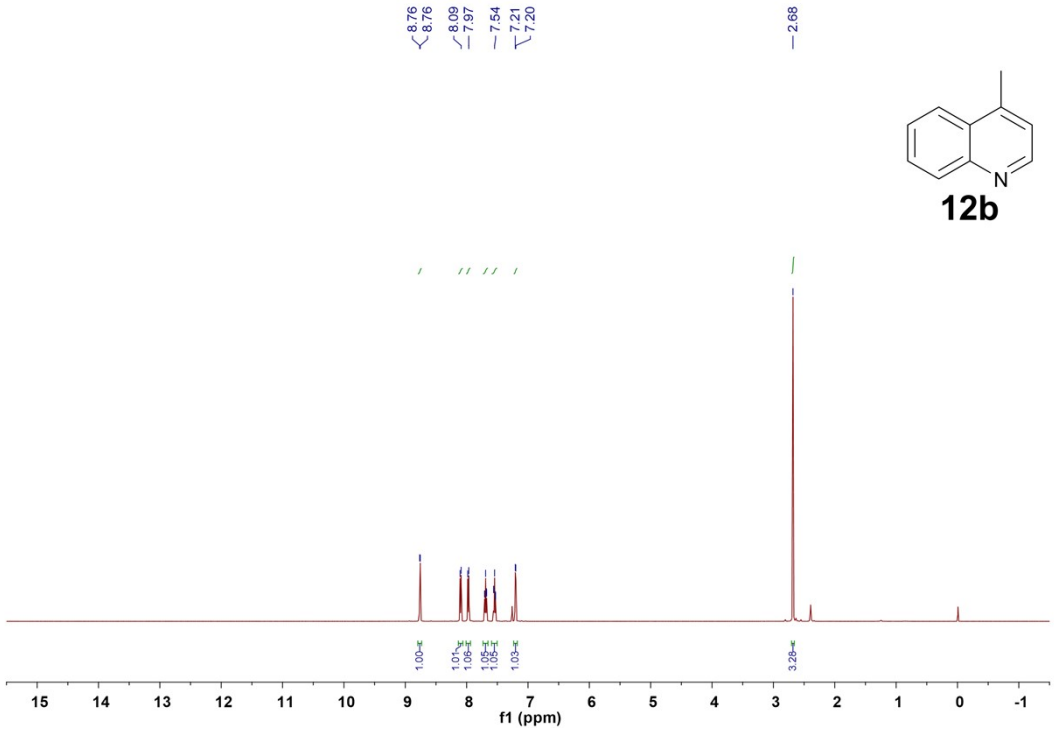

Figure S15. [1]H-NMR spectrum of **12b**

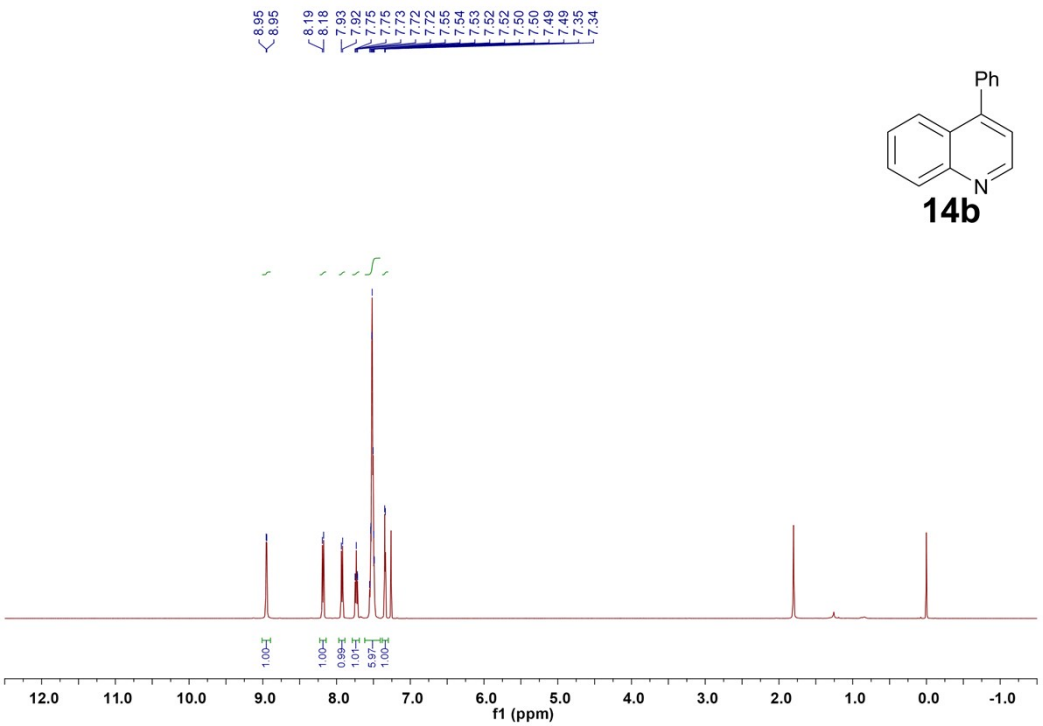

Figure S16. [1]H-NMR spectrum of **14b**

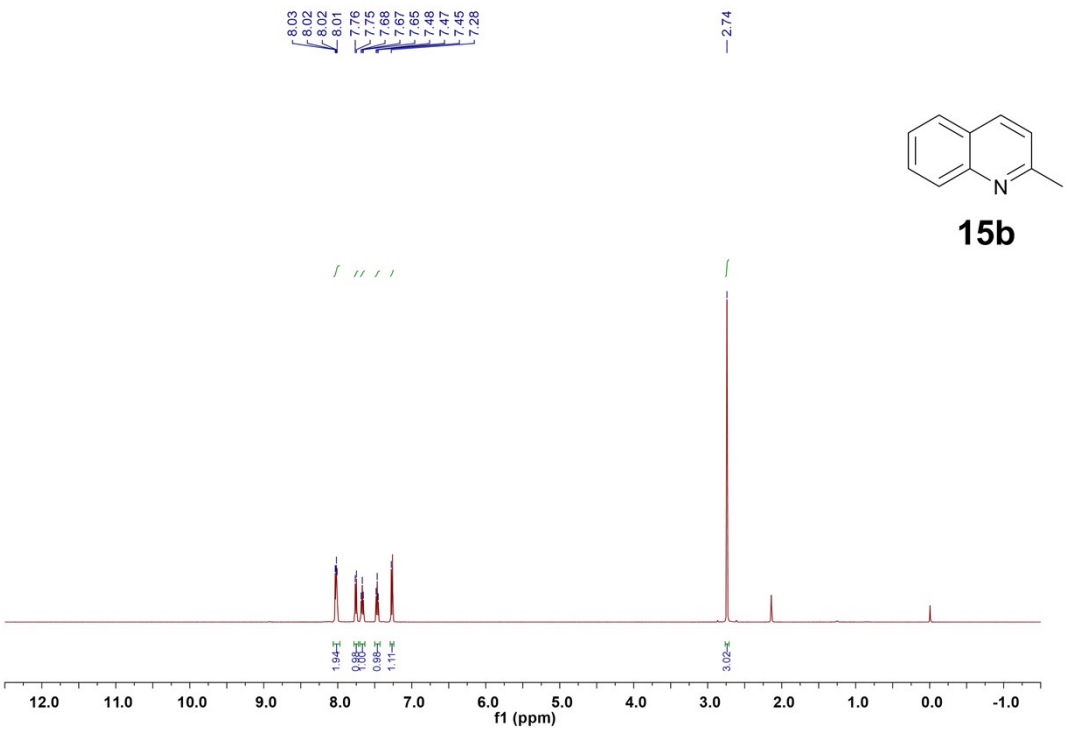

Figure S17. ^{1}H-NMR spectrum of **15b**

3. Preparation and characterization of 1b, 3b and 12b

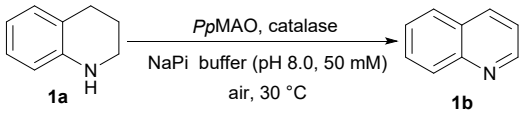

Scheme S1. *Pp*MAO catalyzed oxidative dehydroaromatization of **1a**.

Quinline (1b):

Colorless liquid; 95% yield (18.4 mg); ^{1}H NMR (500 MHz, $CDCl_3$) δ: 8.90 (dd, *J* = 4.2, 1.7 Hz, 1H), 8.14 – 8.08 (m, 2H), 7.78 (dd, *J* = 8.3, 1.4 Hz, 1H), 7.71 – 7.67 (m, 1H), 7.53 – 7.49 (m, 1H), 7.36 (dd, *J* = 8.3, 4.2 Hz, 1H) ppm. ^{13}C NMR (126 MHz, $CDCl_3$) δ: 150.5, 148.3, 136.1, 129.5, 128.3, 127.8, 126.6, 121.1 ppm.

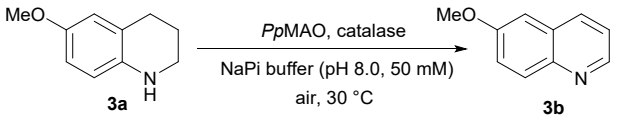

Scheme S2. *Pp*MAO catalyzed oxidative dehydroaromatization of **3a**.

6-Methoxyquinoline (3b):

Yellow liquid; 90% yield (21.5 mg); ^{1}H NMR (500 MHz, $CDCl_3$) δ: 8.72 (dd, *J* = 4.3, 1.7 Hz, 1H), 8.00 – 7.95 (m, 2H), 7.33 (dd, *J* = 9.2, 2.8 Hz, 1H), 7.29 (dd, *J* = 8.3, 4.2 Hz, 1H), 7.00 (d, *J* = 2.8 Hz, 1H), 3.87 (s, 3H) ppm. ^{13}C NMR (126 MHz, $CDCl_3$) δ: 157.7, 147.9, 144.4, 134.8, 130.9, 129.3, 122.3, 121.4, 105.1, 55.5 ppm.

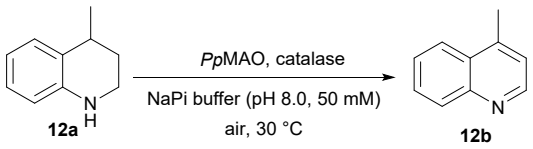

Scheme S3. *Pp*MAO catalyzed oxidative dehydroaromatization of **12a**.

4-Methylquinoline (12b):

Yellow oil; 87% yield (18.7 mg); ^{1}H NMR (500 MHz, $CDCl_3$) δ: 8.75 (d, *J* = 4.3 Hz, 1H), 8.09 (d, *J* = 8.4 Hz, 1H), 7.96 (d, *J* = 8.3 Hz, 1H), 7.70 – 7.66 (m, 1H), 7.56 – 7.51 (m, 1H), 7.19 (d, *J* = 4.3 Hz, 1H), 2.66 (s, 3H) ppm. ^{13}C NMR (126 MHz, $CDCl_3$) δ: 150.2, 148.0, 144.3, 130.1, 129.2, 128.3, 126.3, 123.9, 121.9, 18.7 ppm.

4. NMR Spectra of 1b, 3b and 12b

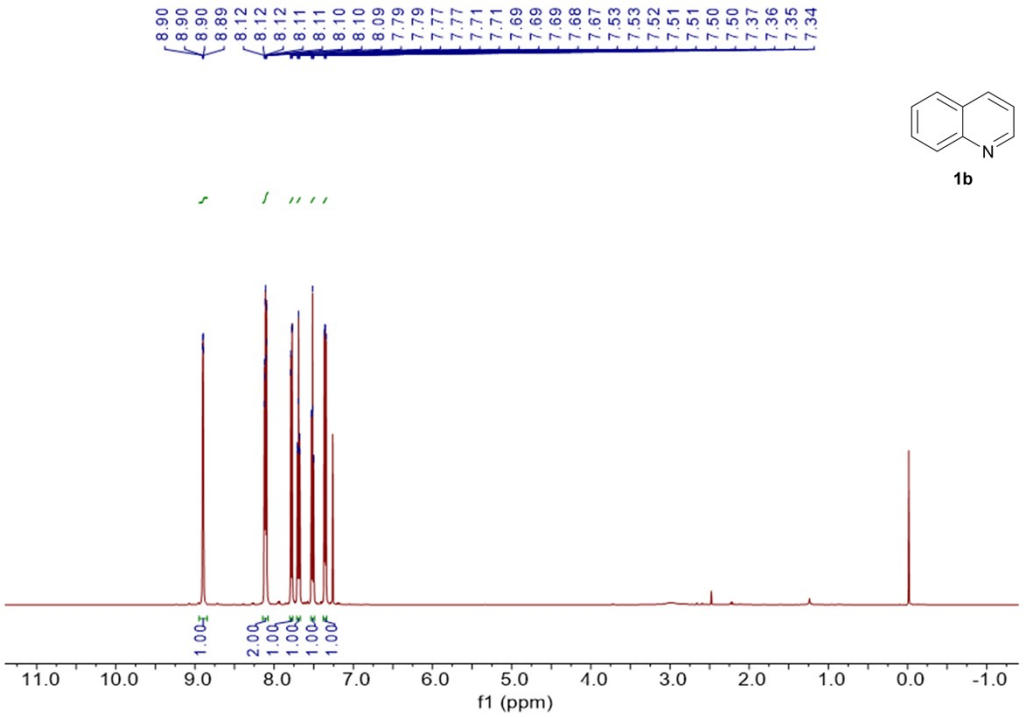

Figure S18. ^{1}H-NMR spectrum of **1b**

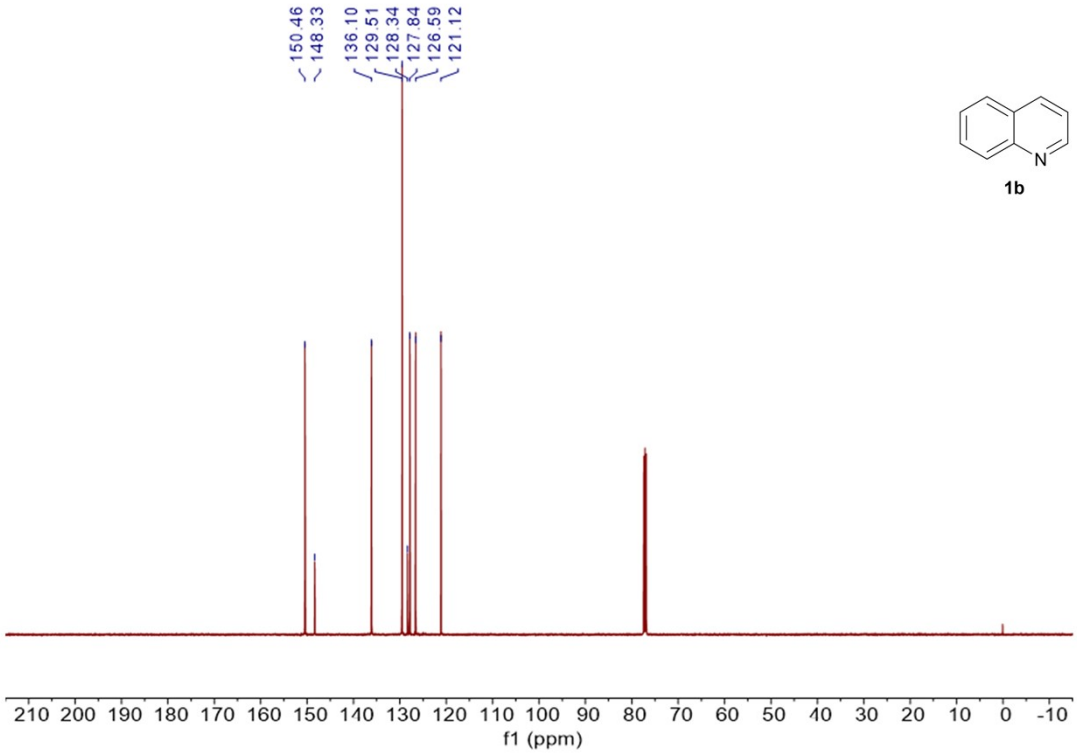

Figure S19. ^{13}C-NMR spectrum of **1b**

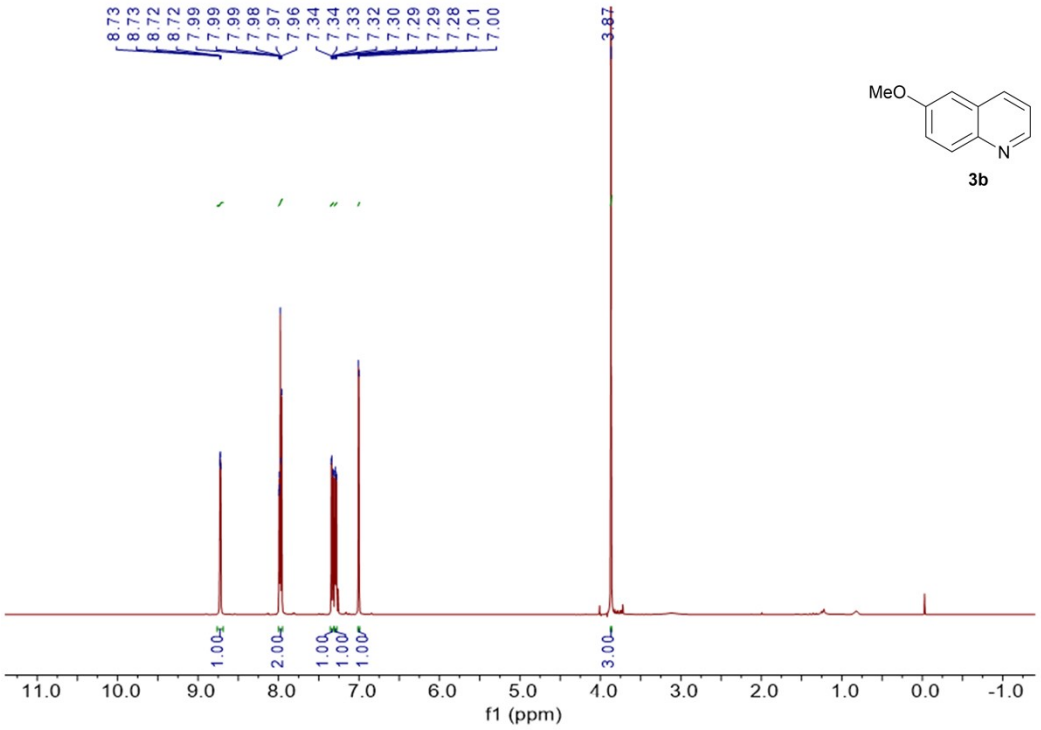

Figure S20. ^{1}H-NMR spectrum of **3b**

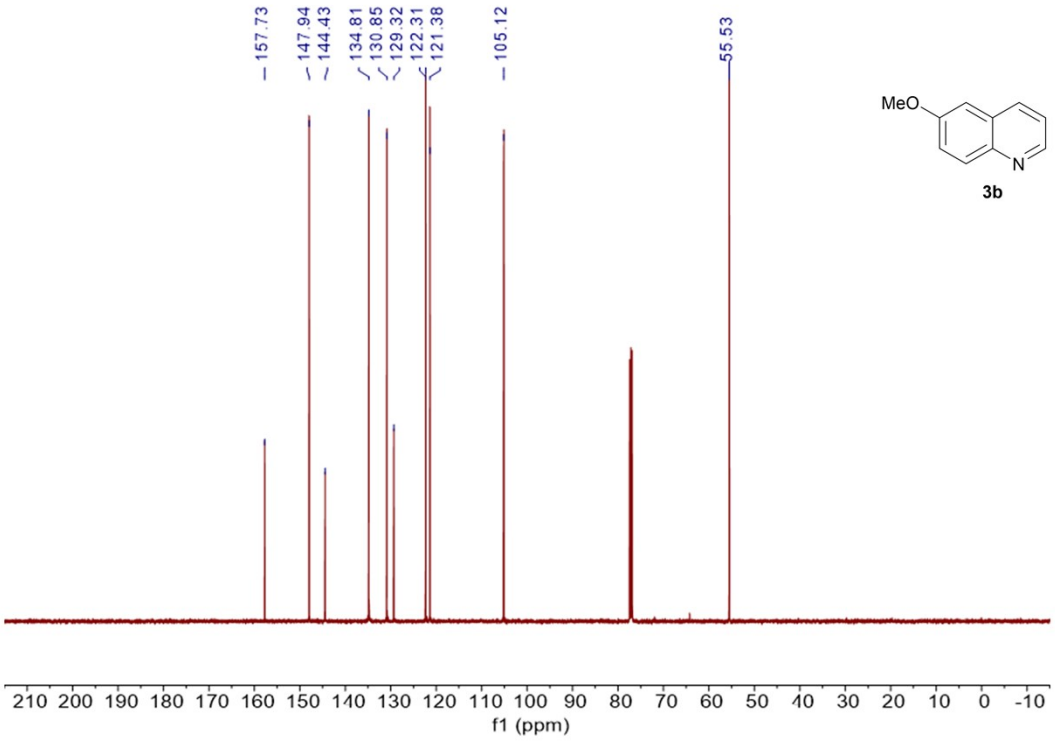

Figure S21. ^{13}C-NMR spectrum of **3b**

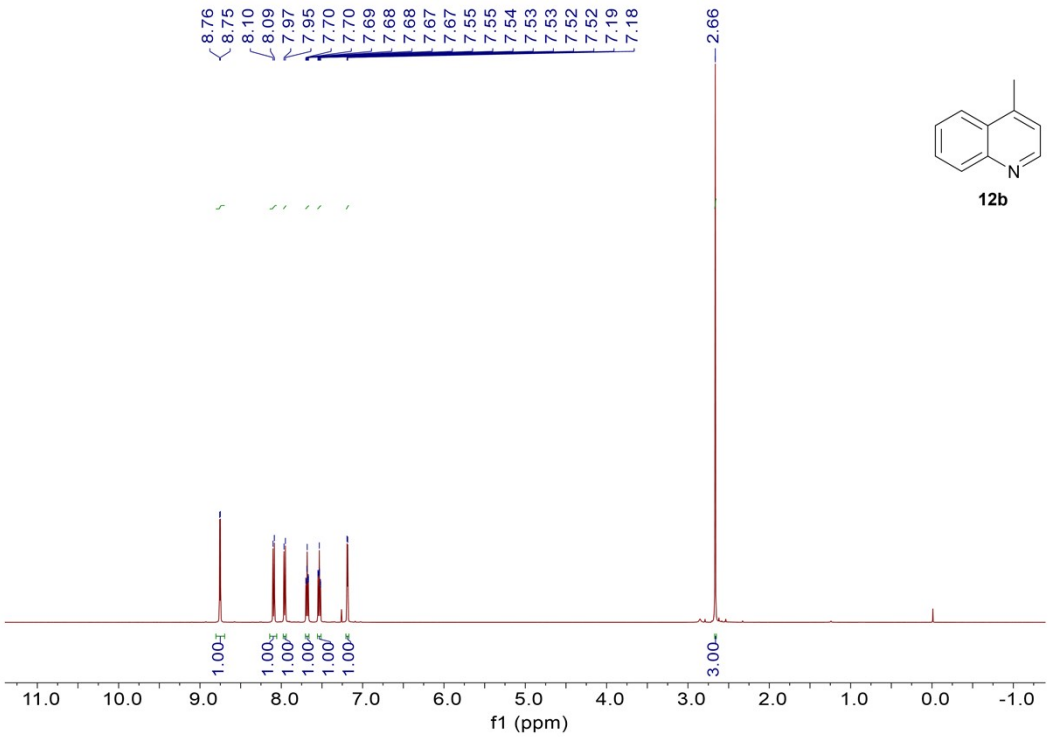

Figure S22. ^{1}H-NMR spectrum of **12b**

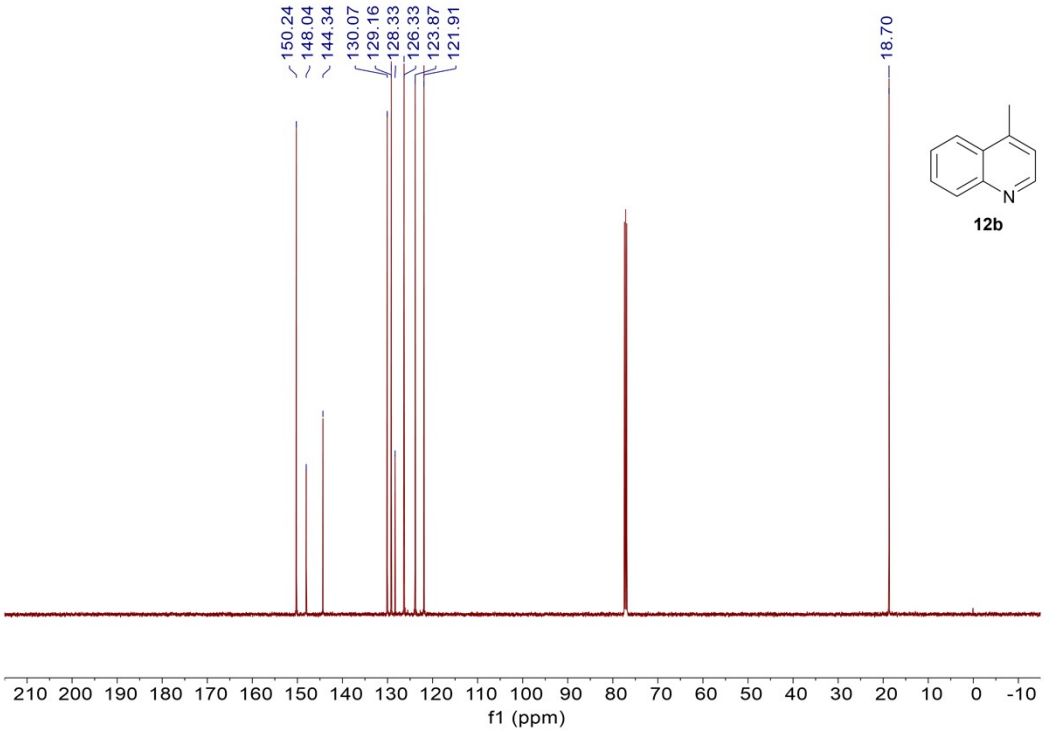

Figure S23. ^{13}C-NMR spectrum of **12b**

5. LC-MS spectrum for mechanism-study of oxidative dehydroaromatization catalyzed by *Pp*MAO

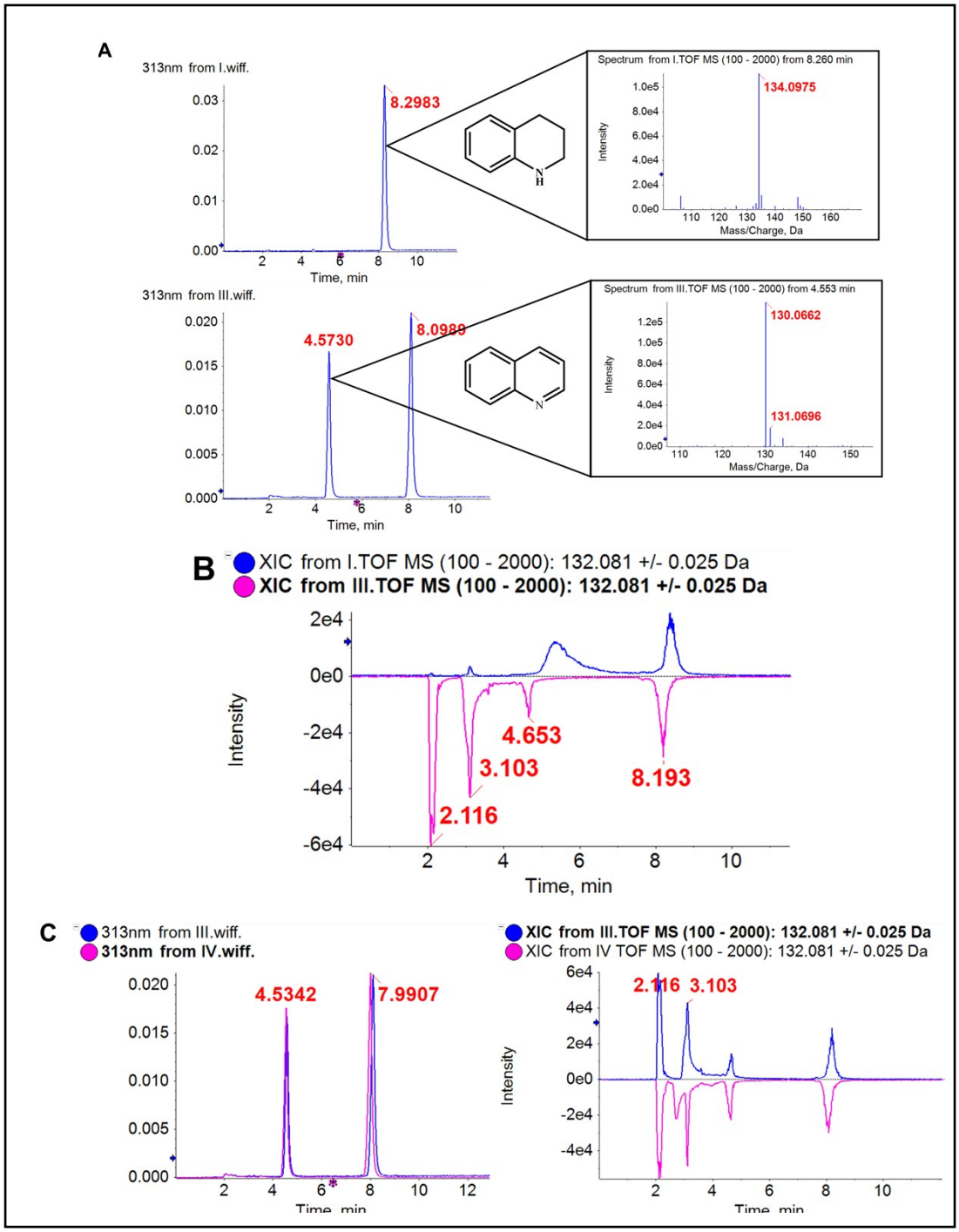

Figure S24. LC-MS analysis of the substrate catalyzed by *Pp*MAO. (A) The analysis showed that the target product quinoline produced by *Pp*MAO with the new peak at m/z 130.0662 and the retention time was 4.5730 min. The insets showed the MS spectra of the substrate and product. (B) A comparison of the extracted ion chromatogram of the imine intermediates between **Ⅰ** and **Ⅲ**. (C) A comparison of the UV spectrum at 313 nm of product and the

extracted ion chromatograms for ions m/z 132.081 (imine intermediate) between Ⅲ and Ⅳ.